Title

Detailed expression profile of all six *Glypicans* and their modifying enzyme *Notum* during chick embryogenesis and their role in dorsal-ventral patterning of the neural tube

Authors

Kawakeb Saad[1], Anthony Otto[1], Susanne Theis[1], Niki Kennerley[2], Andrea Munsterberg[2], Graham Luke[1], Ketan Patel[1,3,*]

Address

1 School of Biological Sciences, University of Reading, Reading, UK

2 School of Biological Sciences, Norwich Research Park, University of East Anglia, Norwich, NR4 7TJ

3 Freiburg Institute for Advanced Studies (FRIAS), University of Freiburg, Freiburg, Germany

Corresponding author ketan.patel@reading.ac.uk

Address

School Biological Sciences

University of Reading

Hopkins Building

Reading

RG6 6UB, UK

Key Words

Embryo, Chick, signalling, Shh, BMP, FGF, Glypican, Notum

Abstract

Vertebrate development is orchestrated by secreted signalling molecules that regulate cell behaviour and cell fate decisions during early embryogenesis. The activity of key signalling molecules including members of Hedgehog, Bone Morphogenetic Proteins and Wnt families are regulated by Glypicans, a family of GPI linked polypeptides. Glypicans either promote or inhibit the action of signalling molecules and add a layer of complexity that needs to be understood in order to fully decipher the processes that regulate early vertebrate development. Here we present a detailed expression profile of all six Glypicans and their modifying enzyme Notum during chick embryogenesis. Our results strongly suggest that these proteins have many as yet undiscovered roles to play during early embryogenesis. Finally, we have taken an experimental approach to investigate their role during the patterning of a key embryonic structure - the neural tube. In particular, we show that over-expression of Notum leads to the dorsalisation of this structure.

Introduction

The development of multicellular organisms is regulated by signalling pathways activated by a diverse range of secreted molecules including wingless (Wnt), Hedgehog (Hh), Bone Morphogenetic Protein (Bmp) and Fibroblast Growth Factor (Fgf) family members. A simplistic view of their action posited that these proteins diffused until they interacted with their receptor to initiate an intracellular signalling cascade, usually culminating in a change of gene expression in the target cell, which then influences cell fate and behaviour.

In the last few years, focus has turned on Heparan Sulfate Proteoglycans (HSPGs) as many genetic studies have demonstrated that they play a central role in regulating signalling during development. HSPGs are abundant cell-surface glycoproteins, which act as co-receptors in signalling processes (Bernfield et al., 1999) and contain one or more covalently attached heparan sulfate (HS) chains (Esko et al., 2009). HSPGs are classified into several families based on their core protein structure. Syndecans, Perlecan and Glypicans (Gpc) are examples of major cell surface HSPGs. Syndecans are transmembrane proteoglycans that contain a highly conserved carboxy-terminal cytoplasmic domain. The HS chains attach to serine residues distal to the plasma membrane. Pelecans are secreted extracellular matrix (ECM) proteoglycans that are not cell-membrane linked. In contrast, Gpcs are attached to the cell surface by a Glycosylphosphatidylinositol (GPI) anchor (Lin, 2004). Gpc core proteins are 60-70 kDa in size and share common structural features across the family. Each Gpc can be divided into three structural domains; the linker domain at the C-terminal end connects the core protein to a GPI anchor in the cell membrane, adjacent to the linker region are the attachment sites for glycosaminoglycan (GAG) chains. The insertion sites are within 50 amino acid residues of the membrane anchor, positioning the GAG chains close to the cell membrane. The third Gpc domain is a globular cysteine-rich domain (CRD) (Pei and Grishin, 2012) .

The tertiary structure of the CRD is thought to remain constant between Gpc family members due to the presence of 14 highly conserved cysteine residues that are predicted to form stabilizing disulphide bonds. Gpc GAG chains are linear sugar polymers consisting of a repeating disaccharide unit. The GAG chains of Gpcs carry a negative charge, allowing promiscuous interaction with basic charged growth

factors (Filmus and Capurro, 2008). Pertinent to the Gpc function is the enzyme Notum since it is able to cleave the former near the cell membrane (Kreuger et al., 2004).

Gpcs have received much attention as they have been shown to modulate the activity of the major classes of secreted proteins that control the development of all animals. The discoveries that mutations in Gpc genes result in diseases such as Simpson-Golabi-Behmel syndrome (Pilia et al., 1996), Omodysplasia (Campos-Xavier et al., 2009) and cancer has brought them into focus (Filmus and Selleck, 2001).

The Gpc gene family members have been conserved during animal evolution and are found in both invertebrates and vertebrates (Filmus et al., 2008; Filmus and Selleck, 2001). There are two Gpc genes in Drosophila: Division abnormally delayed (Dally) and Dally-like protein (Dlp) (Khare and Baumgartner, 2000; Khare et al., 2000), whereas six Gpcs have been identified in mammals (Gpc1 to Gpc6) (Song and Filmus, 2002).

Based on amino acid homology, mammalian Gpcs can be subdivided in two distinct groups. The first group including Gpc1, Gpc2, Gpc4 and Gpc6 with 35%-63% sequence similarity; the second include Gpc3 and Gpc5, which show 54% similarity (Veugelers et al., 1999), whereas the homology between of the two groups is only 17%-25%. The role of Gpcs in modulating signalling activity of secreted proteins is context dependent. In some cases Gpcs can promote the activity of the signalling molecule; for example Gpc3 binds to Wnt proteins and the Wnt receptor Frizzled, to either facilitate or stabilise the complex (Capurro et al., 2014). However, in other situations they attenuate signalling activity; for example Gpc3 inhibits Shh signalling by promoting ligand endocytosis (Capurro et al., 2008).

A number of studies have documented the expression of Gpc or Notum during vertebrate development (Luxardi et al., 2007; Niu et al., 1996; Ybot-Gonzalez et al., 2005), however to our knowledge none have reported a comprehensive profile of all Gpcs and Notum over the entire period of early embryogenesis. Here we provide a detailed expression profile of all Gpcs and Notum during chick embryogenesis starting at the stage of axial mesoderm formation to late limb bud stages (HH-4 to HH-26) (Hamburger and Hamilton, 1951). We show that each gene has its unique expression profile that is temporally highly dynamic. Some Gpcs show strong expression in multiple sites whereas others are more restricted. We show that many are expressed at key patterning sites including Hensen's Node, the notochord, and the floor and roof plates of the neural tube. Finally, we show an important role for Gpcs during the dorsal ventral patterning of the neural tube through the over-expression of Notum, which culminated in a dramatic dorsalisation of key cell determinant markers.

Methods

Cloning of chick Glypican and Notum genes

cDNA was prepared from RNA extracted from whole HH-25 chick embryos. RT-PCR was performed using the following gene specific primers.

cGPC1 F5'-3'GCGAATCTGTCCGCAAGGCTACAC,

R 3'-5'CTAAGCCGTCCCCCATCACTTCAG amplification product size of 1136bp.

cGPC2 F5'-3'GGCAAAAGAAGCAGCAGAGCCTGTTAAAG,

R3'-5'TCATCACCAGGTCTCCATCACACAGC amplification product size of 828bp.

cGPC3 F5'-3'CTGCTCGAGGAGGATGGAGGAGAAGTAC,

R3'-5'CTGTACCTCTCCACGACTTCTTGCCC amplification product size of 1083bp.
cGPC4 F5'-3'GCGACCACTTGAAAGTCTGCTCACAAG,
R3'-5'GCTGCTTGTGATAAACCGCTACTGGG amplification product size of 1400bp.
cGPC5 F5'-3'GAAAGTTTTCCAGCTGCGTCAGCTCG,
R3'-5'GGCAAGGGTTTCTTCGCTGTCTCTTG amplification product size of 1042bp.
cGPC6 F5'-3'TTCTTGCAATTCCAGGGGAACATTTGAG,
R3'-5'ATCCAAACTTGTGCCAGCAGCAGTTG amplification product size of 1001bp.
cNotum F5'-3' ATGCCTTCATGGGAGCGCTGATC,
R3'-5' AACTGGTCCCTGATAGTGGGGCACG amplification product size of 768bp
PCR products were cloned into pDRIVE vector.

Preparation of embryos

All experiments were performed on *Gallus gallus domesticus* chicken embryos. Fertilised eggs were purchased from Henry Stewart and Co, UK. Eggs were incubated at 38ºC and 80% humidity.

Whole mount in-situ hybridisation

Whole mount in-situ hybridisation was performed according to Nieto (Nieto et al., 1996). A minimum of 5 embryos were processed for each experimental outcome reported here.

Cryosectioning

Embryos were washed 3 times with PBS for 15 minutes to remove fixative and equilibrated in 5, 15 and 30% (w/v) sucrose in PBS overnight at 4ºC before freezing in Optimum Cutting Temperature embedding media (O.C.T. Leica Microsystems). 30 µm sections were cut using a cryostat (Bright instruments UK).

Photography

Whole mount embryos were photographed using a Nikon CoolPix camera mounted on a Nikon dissecting microscope. Processed cryo-sections were photographed using an Axiocam digital camera fitted on a Zeiss Axioscope fluorescent microscope connected with Zeiss Axiovision computer software version 3. Images were processed using Adobe Photoshop Elements 6.

Electroporation

Mouse Notum (mNotum) clone was gift from Jorge Filmus (University of Toronto Canada) in pTREACER-FEV5-HisAvector. The mNotum insert was excised with NcoI and XbaI restriction enzymes, and then cloned to the pSLAX vector. Notum insert was cut out from pSLAX with NotI and XbaI then cloned into pCAB5 vector (designed by Jon Gilthore and constructed by Allison Hunter - MRC Centre for Developmental Neurobiology, UK). It contains the beta-actin promoter and an IRES to express GFP from the same backbone.

Eggs were incubated for 2 days to reach HH stage 10-12. Electroporation mixture was made of Carboxymethyl cellulose (CMC), 1% fast green in PBS. The electroporation mixture was prepared by dissolving 0.5 g of CMC in 25ml water and then adding 15 ml of 10XPBS. Once the CMC was completely dissolved, 105 µl of 100 mM MgCl was added. The solution was aliquoted in 400 µl volumes. Thereafter, 75 µl of Fast Green was added to each aliquot. 2 µg of DNA was added to the electroporation mixture in ratio of 1:2. A capillary needle was loaded with prepared DNA/Fast Green mix, which was injected into lumen of the neural tube until the dye filled the entire space using Eppendorf Femtojet Express Microinjector (Eppendorf, UK). PBS solution containing penicillin–streptomycin was dropped on the newly injected manipulation site. Electrodes were positioned to the left and right of the

embryo. Four pulses of 30 milli-seconds at 15 Volts were applied using an Intracel TSS 20 electroporater (Micro Control Instruments, UK) to enable DNA transfection into one half of the neural tube. Eggs were sealed and re-incubated at 37°C and 80% humidity for 16-24 hours. Surviving embryos were investigated for GFP expression using Zeiss Axioscope fluorescent microscope and an Axiocam digital camera. Embryos showing GFP expression were fixed in 4% PFA/PBT and stored at 4°C for further analysis.

Fluorescence microscopy and image analysis

Sections stained with fluorescent secondary antibodies were analysed using a Leica DM4000B fluorescent microscope. Pictures were taken using a DC500 camera system and JPEG formatted images were overlaid if necessary using Leica image analysis software. Minor adjustments to brightness and contrast were made using Adobe Photoshop 6 elements.

Statistical analysis

Data were processed for statistical significance using independent samples t-test at the 95% confidence interval. All data are presented as means and standard errors of the mean (S.E.M).

Results

Expression of *GPC1-6* at HH-4

In order to understand Glypicans (abbreviated henceforth to Gpc) and Notum function during embryonic development in-situ hybridization was used to detail the expression of these genes during development of the chick embryo.

At stage HH-4, *Gpc1* was expressed from the anterior to the posterior of the embryo along the midline (Fig. 1A). The expression was strong in the head process,

Hensen's node and primitive streak. Transverse section through the head process region (Fig. 1A') showed that *Gpc1* was strongly expressed in the ectoderm of the head fold and it became weaker in the ingressing mesoderm (Fig. 1A'''). Transverse section at the level of Hensen's node (Fig. 1A'') showed that *Gpc1* was expressed strongly in the ectoderm as well as the Node.

Gpc2 expression at HH-4 was found in low levels in the anterior part of the embryo (Fig. 1B). Transverse section through the Hensen's node (Fig, 1B') showed that *Gpc2* was weakly expressed in the epiblast and mesoderm. Transverse section though the primitive streak (Fig. 1B'') showed that *Gpc2* was expressed in the ingressing cells in the primitive streak but to a lesser level in tissue that had completed this process.

Gpc3 was expressed in the head process region, Hensen's node, primitive streak at HH-4 (Fig. 1C). Transverse section in the area of head process (Fig. 1C') demonstrated strong expression in the ectoderm. Transverse sections at the level of Hensen's node (Fig. 1C'') showed low level *Gpc3* expression in the ingressing cells.

Gpc4 was expressed strongly in the anterior and posterior most parts of the embryo (Fig. 1D). At Hensen's node (Fig. 1D') *Gpc4* was expressed in the epiblast and the ingressing cells. In the primitive streak *Gpc4* was strongly expressed in the ingressing mesoderm (Fig. 1D''). *Gpc5* was expressed at HH-4 along the primitive streak, Hensen's node and weakly at the anterior of the primitive streak. The expression extended from the primitive streak to the area pellucida (Fig. 1E). Interestingly, its expression in the ectoderm and epiblast was punctate (Fig. 1E'-E'''). *Gpc6* displayed very low level expression (Fig. 1F) but was most prominent at the epiblast immediately adjacent to Hensen's Node (Fig. 1F').

In summary at HH-4, *Gpc1, Gpc4* and *Gpc5* were expressed widely and robustly contrasting *Gpc2, Gpc3 and Gpc6* which were found at low levels.

Expression of *Gpc1-6* at HH 7-8

At HH-7 *Gpc1* was strongly expressed in the head fold, head process, Hensen's node and primitive streak (Fig. 2A). Most striking was the segmental pattern immediately anterior to Hensen's Node. *Gpc1* expression was at low levels in the prechordal plate mesoderm. *Gpc1* was expressed strongly in the neural plate (Fig. 2A'), and primitive streak (Fig. 2A'') both in the epiblast and ingressing cells.

At HH7+, *Gpc2* showed limited expression at HH-7- at the anterior part of the embryo, in the head process region and in Hensen's Node (Fig. 2B and 2B'). *Gpc3* was strongly expressed in the anterior part of the embryo and the head fold at HH-7 (Fig. 2C). Transverse section in the head fold region (Fig. 2C') showed *Gpc3* expressed in the neural tube. *Gpc3* expression in the epiblast at the level of Hensen's Node was particularly strong (Fig. 2C'').

Gpc4 was expressed strongly in the head fold, somites, Hensen's Node and primitive streak at HH-8. Future head region showed strong expression in the neural plate and head ectoderm (Fig. 2D').

At HH-7 *Gpc5* was expressed widely in the developing embryo. Expression was high in the head fold, Hensen's node and primitive streak. At the level of Hensen's Node it was found in the epiblast and mesoderm (Fig. 2E'').

At HH-7 *Gpc6* was expressed at low levels in the head process (Fig. 2F). Low levels of *Gpc6* expression were detected in the neural tube (Fig. 2F'). At the level of Hensen's node *Gpc6* was expressed in the epiblast (Fig. 2F'').

The expression of *Gpc1-6* at HH-12

Gpc1 at HH-12 showed robust expression especially in the anterior and posterior of the gastrulated embryo (Fig. 3A). In the anterior portion of the embryo it was expressed the head mesenchyme, hindbrain and otic placode (Fig. 3A'). *Gpc1* also found in keel of the pharynx (Fig. 3.A'). More posteriorly it was expressed the neural tube, notochord and dermomyotome (Fig. 3A''). *Gpc1* was however stronger in the somites and notochord at the posterior of the embryo (Fig. 3A'''). Low levels of the gene were detected in the intermediate and lateral plate mesoderm.

Similar to *Gpc1*, *Gpc2* at the same stage was expressed strongly in the anterior of the embryo especially the fore, mid and hind brain (Fig. 3B). Also *Gpc2* was expressed in the newly formed somites. Transverse section at the level of the forebrain showed expression of *Gpc2* in neural tube and head mesenchyme (Fig. 3B'). Transverse section at the level of the hindbrain indicated that *Gpc2* was expressed in the neural plate and head mesenchyme. Also it was expressed strongly in the ectodermal floor of the pharynx (Fig. 3B''). Transverse section at the level of the first differentiated somite (Fig. 3B''') showed that *Gpc2* expression was found in sclerotome and lateral plate mesoderm.

Expression of *Gpc3* at HH-12 was restricted to the anterior part of the developing embryo (Fig. 3C). *Gpc3* was expressed in the mid and hindbrain (Fig. 3C) and the anterior tip of foregut (Fig. 3C').

Gpc4 was widely expressed in the developing embryo at HH-11 with striking expression in the fore, mid and hindbrain, neural tube and both undifferentiated and differentiated somites (Fig. 3D). At the level of differentiated somites, it was expressed both in the dermomyotome and sclerotome. These views also revealed expression in the intermediate and lateral plate mesoderm (Fig. 3D'''). *Gpc4* was

also expressed in the roof plate and floor plate and at low levels in the notochord (Fig. 3D’’’).

At HH 10-11 *Gpc5* was expressed throughout the whole embryo and especially strongly in the head region, somites and primitive streak (Fig. 3E). Transverse section in the head region showed that *Gpc5* was strongly expressed in the neural tube (Fig. 3E’’); with weaker expression in the head mesenchyme. Furthermore *Gpc5* was heavily expressed in the keel of the pharynx. Transverse section at the level of differentiated somites showed that *Gpc5* was expressed in the neural tube (Fig. 3E’’). Also some faint expression was found in the splanchnic lateral plate mesoderm. *Gpc5* was expressed in the somites (Fig. 3E’’’).

Gpc6 expression at HH-12 was restricted to the all three compartments of the developing brain (Fig. 3F and F’).

In summary at stage HH10-12 *Gpc1*, *Gpc4* and *Gpc5* expression was prominent in neural tube and somites. On the other hand *Gpc2* and *Gpc3* were restricted to only the anterior part of the chick embryo.

Expression of *Gpc1-6* at HH 18-19

By HH-19 *Gpc1* was expressed in head region, the fore, mid, and hind-brain (Fig. 4A). *Gpc1* was expressed in fore and hind limb buds and was strongly expressed in the Apical Ectodermal Ridge (AER) of the hind limb. *Gpc1* was found in the first and second pharyngeal branches. Transverse section at the level of cranial somites (Fig. 4A’) showed that *Gpc1* was expressed in the neural roof plate and the myotome. Transverse section through the forelimb bud region showed that *Gpc1* was expressed in the neural roof plate and myotome (Fig. 4A’’). Also *Gpc1* was

expressed in the forelimb mesenchyme. In the hind limb (Fig. 4A''') it was expressed in limb bud ectoderm.

By stage HH-19 *Gpc2* had become more restricted in the head and occipital region. There was some expression in the anterior intestinal portal (Fig. 4B). Transverse section in the head region shows expression in the lateral side of the lens vesicle and nasal placode (data not shown). Transverse section in the cranial somite (Fig. 4B') showed expression in the neural floor plate and endoderm. At fore limb level (Fig. 4B'') expression was found in the floor plate and fore limb bud mesenchyme. Furthermore *Gpc2* was expressed in the heart region (Fig. 4B'').

By HH 18 *Gpc3* was expressed in the anterior part of developing embryo (Fig. 4C) with expression in the forebrain, first and second branchial arches, and anterior intestinal portal. *Gpc3* was expressed in the posterior part, the mesoderm of the inter limb region and in fore and hind limb bud. The head region shows *Gpc3* expression in the upper part of the neural tube and distal part of the optic cup. At the cranial somite level *Gpc3* was expressed in the middle of the neural tube (Fig.4C').

Gpc3 expression was detected in the fore limb bud mesenchyme and splanchnic mesoderm (Fig4 C''). In the hind limb it was expressed in the limb mesenchyme and in the lining of embryonic coelom (Fig. 4C''').

At HH-19 *Gpc4* was widely expressed in the embryo. Fig. 4D shows expression the first, second and third branchial arches, and differentiated as well as epithelial somites. In addition, *Gpc4* was expressed in the fore and hind limb buds. Transverse section through the cranial somite showed expression in the neural tube, sclerotome and dermomyotome (Fig.4D'). At the fore limb (Fig.4D'') and hind limb level (Fig. 4D''') expression was found in the neural tube, dermomyotome and sclerotome. *Gpc4* was expressed strongly and in the intermediate mesoderm.

Gpc5 expression at HH-19 had become limited to the posterior part of the embryo. The lateral view of the embryo showed that *Gpc5* was expressed strongly in the fore-limb bud; inter-limb region and hind limb bud (Fig.4E). Transverse section at the forelimb bud level showed expression in the forelimb mesenchyme and weak expression in the neural tube (Fig.4E'). Transverse section through the inter-limb region (Fig. 4E'') showed strong expression in the lateral plate mesoderm and more posteriorly in the hind limb bud mesenchyme (Fig. 4E'''). *Gpc6* expression at HH-19 was limited to the otic placode (Fig. 4F).

***GPC1-6* expression at HH-22**

Lateral view of an embryo at HH-22 showed that *Gpc1* was widely expressed at this stage (Fig.5A) including fore, mid, and hindbrain. Expression was also detected in the first, second and third branchial arches and was strongly expressed in the fore and hind limb buds. Transverse section through the cranial somite (Fig. 5A') showed that *Gpc1* was expressed in the dermomyotome (Fig. 5A'). Transverse section at the forelimb region showed that *Gpc1* expression was localised in both sclerotome and dermomyotome forelimb mesenchyme (Fig. 5A''). *Gpc1* expression in the hind limb AER and dorsal limb ectoderm was prominent as well as in the dorsal root ganglia (Fig. 5A''').

At HH-22 *Gpc2* was still strongly expressed in the anterior part of the embryo especially in the head and neck (Fig. 5B). *Gpc2* was weakly expressed in the posterior part of the embryo, and at low levels in the hind limb and tail bud. Transverse section through the cranial somite (Fig. 5B') showed that *Gpc2* expression was in the ventral part of the neural tube adjacent to the floor plate (Fig. 5B'). Transverse section at the level of the forelimb bud showed that *Gpc2*

expression was found in the intermediate mesoderm as well as the distinct region adjacent to the floor plate (Fig. 5B'' and 5B''').

Lateral view of a HH-22 embryo (Fig. 5C) showed that *Gpc3* was strongly expressed the fore, midbrain and cranial placodes. Transverse section of the cranial somites (Fig. 5C') showed weak *Gpc3* expression in the dorsal root ganglia (Fig. 5C').

The neural tube showed expression under the roof plate at the level of the fore limb (Fig. 5C''). There was strong expression in the forelimb bud mesenchyme. Similar expression was found at the hind limb level (Fig. 5C''').

At HH-22 (Fig. 5D) *Gpc4* was widely expressed the head region, eye and strongly expressed in the midbrain and hindbrain. *Gpc4* expression was found in the branchial arches and in the fore and hind limb buds. Transverse section at the head region showed that *Gpc4* was expressed in the head ectoderm. Transverse section at the cranial somite region showed expression in the dorsal neural tube (roof plate) and dermomyotome (Fig. 5D') both of which extended along the posterior axis. In both fore and hind limbs, *Gpc4* expression was found only in the dorsal mesenchyme (Fig. 5D'' and D''').

At HH-22 *Gpc5* expression was detected at low levels in the fore, inter and hind limb regions (Fig. 5E). Transverse section through the forelimb bud showed that *Gpc5* transcription was weakly expressed in the DRG and also in the limb mesenchyme (Fig.5E''). More posteriorly it was expressed in the hind limb bud mesenchyme and sclerotome (Fig.5E''').

At HH-stage 22 *Gpc6* expressions was solely expressed in the otic placode (Fig.5F).

The expression of *Gpc1-6* at *HH* 24-25

At HH-24 *Gpc1* was expressed in the head region; the frontal nasal process and the branchial arches (Fig. 6A). *Gpc1* was found in the cranial somites and expression become stronger in the trunk somites (Fig. 6A).

Gpc2 was strongly expressed in the first branchial arch and in limb buds. It was expressed strongly in the proximal fore and hind limb buds in contrast to its weak expression in the distal part (Fig. 6B).

Gpc3 expression at HH-24 had become exquisitely limited to the mesenchyme adjacent to the dorsal-ventral interface of the limb buds (Fig. 6C).

At HH-24 *Gpc4* was expressed widely; in the branchial arches region, and highly expressed in the cranial somites and trunk somites (Fig. 6D). It was strongly expressed in the caudal and tail bud somites. However *Gpc4* expression had decreased in the head region. At HH-24 *Gpc5* expression became limited and less intense. There was some expression in the frontal nasal process and bronchial arch regions (Fig. 6E). By HH-25 *Gpc6* was expressed very weakly except for the otic placode and heart (Fig. 6F).

***Notum* expression at stage HH4-7**

Notum was expressed along the entire primitive streak at HH-4 with expression being located predominantly in the epiblast (Fig. 7A-D). By HH-7 (Fig. 7A') *Notum* was expressed in the head fold region, segmenting paraxial mesoderm as well as the Hensen's node region (Fig. 7A'), Transverse section at the segmenting mesoderm level showed that *Notum* was expressed in the notochord and mesoderm undergoing somite formation (Fig. 7C'). In contrast it was weakly expressed in the neural tube (Fig. 7B'). Strong *Notum* expression was detected in ectoderm and in the notochord in the posterior of the post-gastrulated embryo. (Fig. 7D').

Notum expression at stage HH10-13

At HH-10**,** *Notum* was expressed in the fore, mid and hind brain, the somites and lateral plate mesoderm (Fig. 8A). The transcription of *Notum* was very strong in the notochord and remaining primitive streak (Fig. 8A). Transverse section in the head region showed expression in the neural tube, neural crest cells, floorplate and notochord (Fig. 8B). Transverse section at the level of the epithelial somites showed that expression through the somatic mesoderm*,* in the neural roof plate and notochord (Fig. 8C). By HH-13 *Notum* was weakly expressed in the mid and hind brain and first and second pharyngeal arches (Fig.8 A'). In contrast, extremely strong expression was found in the somites, notochord and to a lesser extend in the neural tube. In the somites, expression was confined solely to the dermomyotome (Fig. 8B', C').

***Notum* expression at stage HH18-26**

At HH-18 *Notum* was robustly expressed in all somites, intermediate mesoderm and in the apical ectodermal ridge of the fore and hind-limb buds (Fig. 9A). Expression of *Notum* was also detected in branchial arches 1-3 (Fig. 9A). Transverse section at the cranial somite level showed *Notum* expression in the dorsal neural tube, notochord and dermomyotome (Fig. 9B). At fore limb level, expression was detected in the AER as well as underlying mesoderm (Fig. 9C), a situation also found in the hind limb (Fig. 9D) and apical ectoderm ridge.

At HH-22, *Notum* was expressed in the first branchial arch, and to a lesser extent in the second and third branchial arches. In addition, *Notum* was strongly expressed in the dorsal somatic region and in the fore and hind limb bud (Fig. 9A'). Transverse sections through the cranial somites showed that *Notum* was strongly expressed in the dermomyotome and the dorsal root ganglions (Fig. 9B'). Weak *Notum* expression

was found in the dorsal neural tube. Transverse section at the level of forelimb bud (Fig. 9.C') showed that *Notum* was strongly expressed in the dorsal ectoderm and adjacent mesoderm of the fore and hind limb and in the AER (Fig. 9C' and 9D').

By HH-26 *Notum* was expressed in all somites and branchial arches as well as the limbs (Fig. 9A''). Transvers section in the cranial region showed *Notum* expression in the dorsal root ganglia (DRG), neural tube and roof plate (Fig. 9B''). At the trunk level, expression was clear in the dermomyotome (Fig. 9C''). Transverse section at the fore limb bud showed *Notum* expression in the AER and in the dorsal limb mesoderm (Fig. 9D'').

Note a more detailed expression of all *Gpcs* and *Notum* in the limbs will be presented in separate study (submitted).

Notum over-expression in the neural tube

The neural tube is patterned along the D-V axis by numerous secreted factors. We have shown that many *Gpcs* and *Notum*, which have been proposed to regulate the activity of secreted factors, are also expressed in this tissue. To establish an overview of the impact of Notum on DV patterning we unilaterally electroporated the full length mouse version of the molecule into the right hand side of HH10-12 chick embryo neural tube for a period of 16-24 h. The expression vector also expressed GFP that allowed us to monitor regions that had been manipulated. Robust GFP expression was seen in the right half of the neural tube (Fig. 10A and C). We determined whether the gene of interest was also expressed and performed in-situ to the mouse homologue of Notum.

To examine the effect of Notum over-expression on neural tube pattering we focused on key markers of the neural tube. Firstly, we examined the expression domains of *Nkx-6.1* which is expressed by the undifferentiated ventral cells and *Pax7* which is

expressed by the dorsal cells. In mock electroporations, i.e. with vector containing only GFP, the DV expression levels of both *Pax7* and *Nkx-6.1* were the same on the manipulated side and the un-operated side (Fig. 10E and G). However, in embryos electroporated with mNotum, there was a statistically significant ventral shift of both *Nkx-6.1* (7%) and *Pax7* (13.5%) (Fig. 10F, H, K and M). In addition, we looked at the effect of mNotum over-expression on the *Shh* expression domain along the DV axis. IMAGE J analysis showed that the *Shh* domain decreased by 8.5% on the operated side (Fig. 10I, J, and M). Therefore, over-expression of Notum affected the dorso-ventral patterning of the chick neural tube, with a shift of Pax7 and Nkx-6.1 domains to more ventral regions.

Discussion

The chick has been used as an experimental model to gain insights into vertebrate embryogenesis for a number of reasons including availability of embryos, its amenability to experimental approaches and clarity of in-situ based expression profiles generated with whole-mount techniques.

Data presented in this paper revealed that *Gpcs* and *Notum* were expressed in a stage and tissues-specific manner during chick embryogenesis. During the early developing stages (HH4-10) *Gpc1, Gpc4, Gpc5* and *Notum* were expressed widely and strongly throughout the developing embryo while *Gpc2* and *Gpc3* were expressed in specific regions and *Gpc6* displayed very weak expression.

The temporally early *Gpcs* and *Notum* expression suggests that these genes play important roles during gastrulation. As development progressed *Gpcs* and *Notum* expression became restricted to specific regions. For example, at stages HH-22 and HH-24 *Gpc2, Gpc3, Gpc5* had become limited to specific tissues, suggesting that

Gpcs may have important functions in the later embryonic developing stages. *Gpcs* and *Notum* may have a central role in the pattering events of embryonic structures, such as the neural tube.

Our data show that *Gpc* expression in specific tissues and structures was correlated with regions that express signalling molecules that are known to be regulated by Gpcs. Fgf4 in mammals and avian embryos is implicated in early developmental processes (Alvarez et al., 1998). Fgfs have important roles in the early developmental stages during mesoderm formation, anterior posterior patterning and neural tissue formation. Data from our current study show that *Gpc1, Gpc4 Gpc5* and *Notum* were detected at HH-4 in the primitive streak and the area around Hensen's node and this is consistent with an in-situ hybridisation study by Shamim *et al*., (1999) which showed that Fgf4 were first detected at HH-3 in the anterior primitive streak and the expression become stronger in the central primitive streak and around Hensen's node (Shamim and Mason, 1999). It is possible that *Gpc1, Gpc4 Gpc5* and *Notum* modulate the expression of Fgfs in these areas during the early developmental process.

We found that *Gpc1, Gpc4, Gpc5* and *Notum* were expressed in the primitive streak and in the Hensen's node area at HH-4 where Wnt-3a, Wnt-5a and Wnt-8c are known to be expressed (Hume and Dodd, 1993). Furthermore, Shh is expressed in Hensen's node with stronger expression on the left side. This structure also expresses Gpc1, *Gpc4*, *Gpc5* and *Notum*. A number of studies have shown that Gpcs serve as co-receptors for Shh (Li et al., 2011). There seem to be two types of *Gpc* expression at early developmental stages; *Gpc1,2,3* are expressed in entire cell populations within a given compartment whereas *Gpc5* shows an intriguing punctate pattern within dorsal tissues. These results show the early ectoderm and epiblast is,

at least at the molecular level a heterogeneous tissue. The properties imbued by *Gpc5* expression in the early dorsal structures remains to be determined but it could be related to cell division as Gpc5 has been shown to promote proliferation. Therefore, the detailed expression profiles presented in this study imply that the Gpc/Notum axis has an important role to play in early chick development.

Somite Patterning

The patterning of the somites is a canonical example of how secreted signalling proteins control cell fate. Classical experiments have shown that newly formed somites are naïve in terms of fate and are instructed into developing dorsal dermis, body muscle or the vertebral column by a host of signals that originate from the floor plate, notochord (both secrete Shh), roof plate (Wnt and Bmps), dorsal ectoderm (Wnts) and lateral plate mesoderm (BMPs) (Schmidt et al., 2004; Wagner et al., 2000). The activities of these molecules are regulated by proteins that act as antagonists including Follistatin and Frizzled family members (Connolly et al., 1995; Lin et al., 2007). Here we show that Gpc and Notum activity also add complexity to the process of somite patterning.

One interesting aspect of *Gpc* expression in the somites is the robust transcription of three of the six *Gpcs* during the initial epithelialisation process (*Gpc1, Gpc4* and *Gpc5*). At this stage there is low level Notum expression. The exact role of the *Gpc* expression in the young somites remains to be elucidated but one intriguing possibility is that it acts to dampen the potency of large numbers of patterning signals produced by neighbouring tissues. We suggest that the relatively small field of cells without such a mechanism would otherwise swamp the entire structure and be unable to translate into the precise orchestrated pattern that eventually emerges.

Another interesting feature highlighted by the somite profiling is the discovery of patterns that do not segregate with cellular compartments. For example, the expression of *Gpc4* is highest in regions immediately adjacent to the neural tube which would at a minimum cover areas of the sclerotome and the dermomyotome.

The expression of *Gpcs* and *Notum* have been poorly documented during early vertebrate embryogenesis. Our study gives a detailed profile of this axis during chick development and in addition highlights some fascinating differences between the expression of chick genes compared to their mouse counterparts. For example, we found that *Gpc4* is robustly expressed during the early stages of chick development in particularly the hind brain and somites. However this is not the same for the mouse homologue where Yboy-Gonzalez and others have shown a much more restricted profile (Ybot-Gonzalez et al., 2005). *mGpc4* appears not only quantitatively different to its chick counterpart but also qualitatively unique in that the chick gene is expressed at sites where the mouse version is not, for example in the dorsal limb mesenchyme. It could be that the qualitative differences could be covered by other family members in the mouse. Detailed expression profiling in mammalian tissues could settle this matter. Most importantly these results suggest that the Gpc/Notum axis has an important role in vertebrate somite development. Indeed a recent study showed a novel mechanism involving the patterning of somites involving neural crest through the action of Gpc4 (Serralbo and Marcelle, 2014).

Neural Tube Patterning

Chick *Gpc* and *Notum* showed a very interesting expression profile in the midline structures; the neural tube and the notochord. Our study showed that these structures expressed *Gpc1, 3, 4* and *5* as well as *Notum*. The later was particularly

interesting as it was expressed in the dorsal neural tube from early stage HH-10 and the expression maintained until later stage HH-26. In the notochord it was expressed from HH-10 to HH-18. This suggests a putative role for Gpcs in neural tube patterning. Several subclasses of neurons are generated at specific dorsal-ventral positions in the neural tube in response to gradient concentrations of Shh expressed by the floor plate. Precise Shh concentration defines the identity of ventral neural progenitor cells by expressing unique combinations of transcription factors (Ericson et al., 1997). In contrast the roof plate and other dorsal tissues secrete members of the BMP and Wnt family of polypeptides to dorsalise the fate of neural tube cells (Altmann and Brivanlou, 2001). Here we show that over-expression of Notum in the neural tube results in its dorsalisation; extension of the expression domain of the dorsal marker Pax7 and reduction in the expression domain of the ventral markers Nkx6.1 and Shh. Over-expression of Notum could change the neural tube landscape by either affecting dorsal or ventral signalling by modulating the action of Gpcs. A huge body of research has demonstrated Gpc modulation of BMP signalling, both in invertebrates and vertebrates (Grisaru et al., 2001; Jackson et al., 1997). Pertinent to this study was the finding by Dwivedi et al who showed that Gpcs inhibit BMP signalling (Dwivedi et al., 2013). Therefore one explanation of the dorsalised neural tube is that the inhibitory action of Gpcs (specifically *Gpc4* and *5*, based on expression profiles) on Bmps is lifted by over-expression of Notum.

Alternatively Notum over-expression could affect the ventralising activity of the floor plate. Again a large body of evidence exists showing that Gpcs promote Shh signalling (Li et al., 2011; Wilson and Stoeckli, 2013) and that Shh expression from the notochord induces the expression of Shh in the floor plate which then patterns the neural tube (Roelink et al., 1994). Therefore it is conceivable that the decrease

in Shh expression we reported after Notum over-expression is due to a disruption of the Shh auto-regulatory cascade underpinned by the Gpcs.

In summary we present the first full detailed profile of *Gpc* and *Notum* expression during chick embryonic development. We show that these genes have unique temperal/spatial expression patterns. Some genes (e.g. *Gpc1, Gpc4* and *Notum*) are expressed at high levels in multiple tissues during the development of the organism whereas others (especially *Gpc6*) are expressed at a few sites at low levels. The study highlights that signalling mechanisms that control all tissue patterning through the action of secreted proteins are going to be regulated by the action of the Gpc/Notum axis.

Legends

Figure 1: Expression pattern of *Gpc1-Gpc6* at HH-4.

(A-F) Whole mount in situ hybridisation *of Gpc1-Gpc6* respectively. Dotted lines indicated the transverses sections planes presented in A'- F''' (A', A'') *Gpc1* expressed in the ectoderm and epiblast respectively (red arrow), (A'') *Gpc1* expression in the ingression mesoderm (red arrow head). (B') *Gpc2* expressed in low level in the ingressing tissue (red arrow). (C') *Gpc3* was expressed in level in epiblast (red arrow). (C'', C''') *Gpc3* expressed in epiblast. (D') *Gpc4* was expressed in the ingressing cells at level of Hensen's Node (red arrow). (D'') *Gpc4* was expressed in the hypoblast (red arrowhead). (E') Punctate *Gpc5* expression in the ectoderm (red arrow). (E''-E''') Punctate *Gpc5* expression in the epiblast (red arrowhead). (F') *Gpc6* was expressed in very low level in the epiblast (red arrowhead). (F''-F''') No *Gpc6* expression in posterior regions.

Figure 2: Expression pattern of *Gpc1-Gpc6* at HH7-8.

(A-F) Whole mounts in-situ hybridisation embryos of *Gpc1* HH-7, *Gpc2* HH-7+, *Gcp3* HH-7, *Gpc4* HH-8, *Gpc 5* HH-7, *Gpc6* HH-7 respectively. Section planes are indicated by black dotted lines. (A'-F'''). (A') *Gpc1* was expressed in the ectoderm (red arrow). (A'') *Gpc1* was expressed in Hensen's Node and ectoderm (red arrow). (B') Detail of anterior expression of *Gpc2.* (C') *Gpc3* expression in the floor of pharynx (red arrow). (C'') *Gpc3* was expression in the ectoderm (neural) (red arrow). (D') *Gpc4* expression in the head fold (red arrow). (D'') *Gpc4* was expressed in the ectoderm (red arrow) and endoderm and mesoderm (red arrow head). (E') *Gpc5*

expression in anterior neural tube. (E'') *Gpc5* expression in high level in the neural plate and ectoderm (red arrow). (F') *Gpc6* expression in the floor of pharynx (red arrow). (F'') *Gpc6* expressed at very low level in the ectoderm (red arrow).

Figure 3: The expression pattern of *Gpc1-Gpc6* at HH10-12.

(A-F) Whole mounts in-situ hybridisation embryos of *Gpc1* HH-12, *Gpc2* HH-12, *Gcp3* HH-12, *Gpc4* HH-11, *Gpc 5* HH-10, *Gpc6* HH-12 respectively. Section planes are indicated by black dotted lines (A'-F''').

(A') Transverse section in the hindbrain, *Gpc1* was expressed in the otic placode (red arrow), and neural tube (red arrowhead), (A'') *Gpc1* expression in the dermomyotome (red arrow head), and notochord (red head). (A''') *Gpc1* expression in the segmental plate (red arrow head) and notochord (red head). (B') *Gpc2* expression in the neural tube (red arrow head), head mesenchyme (red arrow). (B'') *Gpc2* expression in the neural tube (red arrow), head mesenchyme (red arrow head), and ectodermal floor of pharynx (black arrow). (B''') Transverse section of differentiated somite depicting *Gpc2* expression in the sclerotome (red arrow). (C') At hind brain level, *Gpc3* expression in the in the anterior tip of foregut (red arrow). (C'') Expression in the heart tube (red arrow). (C'') Somites failed to express *Gpc3.* (C''') No expression in posterior. (D') *Gpc4* expression in the hind brain (red arrow) and in the head mesenchyme (red arrowhead), (D'') *Gpc4* expression in the neural tube (red arrow), in the thick walled floor of pharynx (red arrow head) and sclerotome (black arrow). (D''') *Gpc4* expression in the roof plate and floor plate (red arrowhead and blue arrowhead) respectively and sclerotome (red arrow), in the lateral plate mesoderm. (E') *Gpc5* expression in the neural tube (red arrow). (E'') *Gpc5* expression in the head mesenchyme (red arrow). (E''') *Gpc5* expression in the

epithelial somite (red arrow). (F'-F'') Weak *Gpc6* expression in the developing brain region (red arrow) but not in the spinal cord part of the neural tube (F''').

Figure 4: Expression pattern of *Gpc1-Gpc6* during HH18-19.

(A-F) Whole mounts in-situ hybridisation embryos of *Gpc1* HH-19, *Gpc2* HH-19, *Gcp3* HH-18, *Gpc4* HH-19, *Gpc5* HH-19, *Gpc6* HH-19 respectively. Section planes are indicated by black dotted lines (A'-F''').

(A) *Gpc1* was expressed in the brain (blue arrow head) and in the fore and hind limb bud (red arrowheads). (A') *Gpc1* expression in the roof plate (red arrow head) and dermomyotome (red arrow). (A'') *Gpc1* expression in the forelimb bud dorsal mesoderm (red arrowhead) and in the dorsal neural tube (blue arrowhead), as well as (A''') in the hind limb bud ectoderm (red arrowhead). (B) *Gpc2* was expressed strongly in the head and neck region (red arrow), (B') dorsal to floor plate (red arrowhead). (B'') restricted expression of *Gpc2* to region adjacent to floor plate (red arrowhead) and in fore limb ectoderm and mesenchyme (red arrow). (B''') Posterior part devoid of *Gpc2* expression. (C) *Gpc3* expression in head placodes (red arrowhead) and limbs hind limb bud (blue arrows). (C') Weak *Gpc3* expression in middle (D-V) neural tube (red arrowhead). (C'') Strong *Gpc3* expression in fore limb ectoderm and mesenchyme (blue arrow) and gut mesoderm (red arrowhead). (C''') Strong *Gpc3* expression in hind limb (red arrow). (D) Strong segmental expression of Gpc4 as well in branchial arches (red arrowhead). (D') *Gpc4* expression in dermomyotome (red arrow) and myotome (blue arrow head). (D'') *Gpc4* expression in the dorsal neural tube (blue arrow), region of somite adjacent to neural tube (red arrow), intermediate mesoderm (green arrow) and proximal fore limb mesoderm (red arrowhead). (D''') *Gpc4* expression in hind limb mesenchyme (red arrow), intermediate mesoderm (green arrow) and throughout young somite (blue

arrowhead). (E) *Gpc5* expression in the fore and hind limb bud (red arrows). (E') *Gpc5* expression in the forelimb bud mesenchyme (red arrow). (E'') Very little expression at inter limb level. (E''') Proximal *Gpc5* expression in hind limb (red arrow). (F) *Gpc6* expression only in the otic placode (red arrow). (F'-F''') Little *Gcp6* expression in body.

Figure 5: Expression pattern of *Gpc1-Gpc6* at HH-22.

(A-F) Whole mounts in-situ hybridisation embryos of *Gpc1- Gpc6 at* HH-22 respectively. Section planes are indicated by black dotted lines (A'-F''').

(A) *Gpc1* was expressed in the head (red arrows), in the fore and hind limb bud (black arrows). (A') Weak *Gpc1* expression in the neural tube (red arrowhead), DRG (blue arrowhead), and dermomyotome (red arrow). (A'') Expression in the fore limb mesenchyme (blue arrow), DRG (blue arrowhead), dorsal neural tube (red arrowhead) and dermomyotome (red arrow). (A''') Expression of *Gpc1* in the dorsal neural tube (red arrowhead), limb ectoderm (blue arrow), AER (red arrow) and ventral body ectoderm (blue arrowhead). (B) *Gpc* expression in head and occipital region (red arrows). (B' and B''') *Gpc2* expression immediately dorsal to floor plate (red arrowhead). (C) *Gpc3* expressed in the head placodes (red arrowheads), fore and hind limb bud (black arrow head). (C') *Gpc3* in the dorsal neural tube (red arrow head) and ventral mesoderm (red arrow). (C'') *Gpc3* expression in the dorsal neural tube (red arrowhead) and fore limb mesenchyme (red arrow). (C''') *Gpc3* expression in the dorsal neural tube (red arrowhead) and hind limb mesenchyme. (D) *Gpc4* expression in somites (red arrows) and branchial arches (red arrowhead). (D') *Gpc4* expression in the roof plate (red arrow head) and dermomyotome (red arrow), (D'') *Gpc4* expression in the roof plate (red arrow head), dermomyotome (red arrow) and

in the fore limb bud mesenchyme (blue arrow). (D''') *Gpc4* expression inn roof plate (red arrow head), dermomyotome (red arrow) and in the sub-ectodermal hind limb bud mesenchyme (blue arrow). (E) *Gpc5* expression in limbs (red arrowheads). (E') *Gpc5* expression in the DRG (red arrow), (E'') *Gpc5* was expression in the forelimb bud mesenchyme (red arrow) and DRG (red arrowhead). (E''') Gpc5 expression in the DRG (red arrowhead) and hind limb mesenchyme (red arrow). (F) *Gpc6* expression in the otic placode (red arrowhead). (F'-F''') Little *Gcp6* expression in body.

Figure 6: Expression pattern of *Gpc1-Gpc6* during HH 24-25.

(A-F) Whole mount in situ embryo for *Gpc1-Gpc5* expression at HH24 and *Gpc6* at HH-25 respectively. (A) *Gpc1* in the fore and hind limb bud (red arrows head). (A') *Gpc1* expressed in the somites (blue arrow) and branchial arch region (red arrow). (B and B') *Gpc2* expression in the branchial arches (red arrow) in the fore and hind limb buds (red arrowsheads). (C) *Gpc3* expression in the somites (red arrow) and fore and hind limb buds (red arrow head). (D) *Gpc4* expression in optics region (red arrow), posterior margin of fore limb (blue arrow) and strong in posterior somites (white arrow). (D') Detail of cervical region showing strong expression of *Gpc4* in dorsal midline (black arrow), somites (red arrow) and branchial arch (blue arrow). (E) *Gpc5* expression in segmental pattern in the body (red arrowhead) and fore and hind limb (red arrow). (E') Detail of *Gpc5* expression in segmental pattern in the cervical region. (F) Expression of *Gpc6* in the heart at HH-25 (F') Detail showing expression ventral to somites in cervical region (red arrows).

Figure 7: *Notum* expression at HH-4-10

(A) Dorsal view of HH-4 and (A') HH-7. Dotted line indicate section plane for B-D and B'-D'. (A) *Notum* expression along the primitive streak and adjacent to the Hensen's Node (red arrow). (B) *Notum* expression in ectoderm (red arrowhead). (C-D) *Notum* expression in epiblast with weak expression in ingressing cells (red arrowhead). (A') Segmental paraxial expression of *Notum.* (B') *Notum* expression in the neural plate (red arrowhead) in head mesenchyme (blue arrowhead). (C') *Notum* expression indicated pre-somitic mesoderm (red arrow), neural plate (red arrowhead) and notochord (blue arrow). (D') Expression of *Notum* epiblast (red arrowhead) and ingressing cells (red arrow).

Figure 8: Expression of *Notum* at HH-10-13

(A) Dorsal view of HH-10 and (A') HH-13 embryo. Dotted line indicate section plane for B-D and B'-D'. (A) *Notum* expressed robustly in the head, somites and midline structures (red arrow). (B) Expression of *Notum* in the neural tube (red arrowhead) and head mesenchyme (red arrow). (C) Expression of *Notum* in dorsal neural tube (red arrowhead), throughout early differentiating somite (red arrow) and notochord (blue arrow). (C) Expression of *Notum* in the notochord (blue arrow) and pre-somitic mesoderm (red arrow). (A') *Notum* robustly expressed in the somites and midline structure (red arrow). (B') Expression of *Notum* in the dermomyotome (red arrowhead and lower levels in sclerotome (red arrow). Strong expression in notochord (blue arrowhead). (C') Weak *Notum* expression in dorsal neural tube (red arrowhead). Strong expression of *Notum* in dorsal region of epithelial somite (red arrow) and notochord (blue arrowhead). (D') *Notum* expression in neural tube (red arrowhead), notochord (blue arrowhead) and pre-somitic mesoderm (red arrow).

Figure 9: *Notum* expression HH-18 to HH-26

(A) Dorsal view of HH-18 (A') HH-22 and (A'') HH-26 embryo. Dotted line indicate section plane for B-D and B'-D'. (A) Expression of *Notum* in the branchial arches, somites, fore and hind limb buds. (B) Expression in in dorsal neural tube (red arrowhead) and dermomyotome (red arrow). (C) Fore limb expression (blue arrow), dermomyotome (red arrow), dorsal neural tube (red arrowhead) ad notochord (blue arrowhead). (D) Hind limb expression (red arrow), dermomyotome (red arrow), dorsal neural tube (red arrowhead) ad notochord (blue arrowhead). (A') Expression of *Notum* in the branchial arches (blue arrow), dorsal structure (red arrow), fore limb (blue arrowhead) and hypaxial somatic region (white arrow). (B') *Notum* in the dermomyotome (red arrow), dorsal neural tube (red arrowhead) and neural crest derived cells (blue arrowhead). (C') Expression in the fore limb dorsal ectoderm and AER (red arrow). (D') Expression in the hind limb dorsal ectoderm and AER (red arrowhead). (A'') Robust expression of Notum in body segments and limbs. (B'') Expression of Notum in epaxial lip (red arrow), around the DRG (blue arrow) and in dorsal neural tube (red arrowhead). (C'') Expression in the dermomyotome (red arrow) and around DRG (red arrowhead). (D'') Expression in dermal sub-ectodermal mesenchyme (red arrow) and AER (red arrowhead).

Figure 10: *Notum* overexpression in the neural tube

(A) Dorsal view chick embryo electroporated at HH-11 and viewed 16h later for showed the GFP expression in the neural tube. (B) Whole mount in-situ hybridisation of embryo electroporated with mouse *Notum* (red arrow). (C) Transverse section in the electroporated area showing unilateral GFP expression. (D) Transvers section in the electroporated embryo showing *mNotum* expression in the neural tube. (E)

Whole mount for *Nkx6.1* and *Pax7* in control electroporated embryo. (G) No change in expression level of Nkx6.1 (blue arrow) or Pax7 (red arrow) in control embryo. Red arrows indicates *Pax7* expression and blue Nkx6.1. Note ventral shift of both in (H). (F) Effect of *Notum* over-expression on Pax7 and Nkx-6.1 expression. (H). Section of mNotum over-expression embryo. Red arrows indicates *Pax7* expression and blue Nkx6.1. Note ventral shift of both markers. (I) Wholemount for *Shh* in mNotum electroporated embryo. (J) Section of mNotum over-expression and *Shh* expression Red arrows indicate *Shh* expression Note ventral shift in *Shh* on right side. (K-M) Dorsal-ventral expression domains (% length) in control and mNotum electroporated embryos of (K) *Nkx6.1*, (L) *Pax7* and (M) *Shh*. Error bars in graphs represent standard error. 3 embryos per treatment were analysed. Asterisk denotes statistical significance where $p < 0.05$.

References

Altmann, C.R., and Brivanlou, A.H. (2001). Neural patterning in the vertebrate embryo. Int Rev Cytol *203*, 447-482.

Alvarez, I.S., Araujo, M., and Nieto, M.A. (1998). Neural induction in whole chick embryo cultures by FGF. Dev Biol *199*, 42-54.

Bernfield, M., Gotte, M., Park, P.W., Reizes, O., Fitzgerald, M.L., Lincecum, J., and Zako, M. (1999). Functions of cell surface heparan sulfate proteoglycans. Annu Rev Biochem *68*, 729-777.

Campos-Xavier, A.B., Martinet, D., Bateman, J., Belluoccio, D., Rowley, L., Tan, T.Y., Baxova, A., Gustavson, K.H., Borochowitz, Z.U., Innes, A.M.*, et al.* (2009). Mutations in the heparan-sulfate proteoglycan glypican 6 (GPC6) impair endochondral ossification and cause recessive omodysplasia. Am J Hum Genet *84*, 760-770.

Capurro, M., Martin, T., Shi, W., and Filmus, J. (2014). Glypican-3 binds to Frizzled and plays a direct role in the stimulation of canonical Wnt signaling. J Cell Sci *127*, 1565-1575.

Capurro, M.I., Xu, P., Shi, W., Li, F., Jia, A., and Filmus, J. (2008). Glypican-3 inhibits Hedgehog signaling during development by competing with patched for Hedgehog binding. Dev Cell *14*, 700-711.

Connolly, D.J., Patel, K., Seleiro, E.A., Wilkinson, D.G., and Cooke, J. (1995). Cloning, sequencing, and expressional analysis of the chick homologue of follistatin. Dev Genet *17*, 65-77.

Dwivedi, P.P., Grose, R.H., Filmus, J., Hii, C.S., Xian, C.J., Anderson, P.J., and Powell, B.C. (2013). Regulation of bone morphogenetic protein signalling and cranial osteogenesis by Gpc1 and Gpc3. Bone *55*, 367-376.

Ericson, J., Rashbass, P., Schedl, A., Brenner-Morton, S., Kawakami, A., van Heyningen, V., Jessell, T.M., and Briscoe, J. (1997). Pax6 controls progenitor cell identity and neuronal fate in response to graded Shh signaling. Cell *90*, 169-180.

Esko, J.D., Kimata, K., and Lindahl, U. (2009). Proteoglycans and Sulfated Glycosaminoglycans.
Filmus, J., and Capurro, M. (2008). The role of glypican-3 in the regulation of body size and cancer. Cell Cycle *7*, 2787-2790.
Filmus, J., Capurro, M., and Rast, J. (2008). Glypicans. Genome Biol *9*, 224.
Filmus, J., and Selleck, S.B. (2001). Glypicans: proteoglycans with a surprise. J Clin Invest *108*, 497-501.
Grisaru, S., Cano-Gauci, D., Tee, J., Filmus, J., and Rosenblum, N.D. (2001). Glypican-3 modulates BMP- and FGF-mediated effects during renal branching morphogenesis. Dev Biol *231*, 31-46.
Hamburger, V., and Hamilton, H.L. (1951). A series of normal stages in the development of the chick embryo. J Morphol *88*, 49-92.
Hume, C.R., and Dodd, J. (1993). Cwnt-8C: a novel Wnt gene with a potential role in primitive streak formation and hindbrain organization. Development *119*, 1147-1160.
Jackson, S.M., Nakato, H., Sugiura, M., Jannuzi, A., Oakes, R., Kaluza, V., Golden, C., and Selleck, S.B. (1997). dally, a Drosophila glypican, controls cellular responses to the TGF-beta-related morphogen, Dpp. Development *124*, 4113-4120.
Khare, N., and Baumgartner, S. (2000). Dally-like protein, a new Drosophila glypican with expression overlapping with wingless. Mech Dev *99*, 199-202.
Khare, N., Fascetti, N., DaRocha, S., Chiquet-Ehrismann, R., and Baumgartner, S. (2000). Expression patterns of two new members of the Semaphorin family in Drosophila suggest early functions during embryogenesis. Mech Dev *91*, 393-397.
Kreuger, J., Perez, L., Giraldez, A.J., and Cohen, S.M. (2004). Opposing activities of Dally-like glypican at high and low levels of Wingless morphogen activity. Dev Cell *7*, 503-512.
Li, F., Shi, W., Capurro, M., and Filmus, J. (2011). Glypican-5 stimulates rhabdomyosarcoma cell proliferation by activating Hedgehog signaling. J Cell Biol *192*, 691-704.
Lin, C.T., Lin, Y.T., and Kuo, T.F. (2007). Investigation of mRNA expression for secreted frizzled-related protein 2 (sFRP2) in chick embryos. J Reprod Dev *53*, 801-810.
Lin, X. (2004). Functions of heparan sulfate proteoglycans in cell signaling during development. Development *131*, 6009-6021.
Luxardi, G., Galli, A., Forlani, S., Lawson, K., Maina, F., and Dono, R. (2007). Glypicans are differentially expressed during patterning and neurogenesis of early mouse brain. Biochem Biophys Res Commun *352*, 55-60.
Nieto, M.A., Patel, K., and Wilkinson, D.G. (1996). In situ hybridization analysis of chick embryos in whole mount and tissue sections. Methods Cell Biol *51*, 219-235.
Niu, S., Antin, P.B., Akimoto, K., and Morkin, E. (1996). Expression of avian glypican is developmentally regulated. Dev Dyn *207*, 25-34.
Pei, J., and Grishin, N.V. (2012). Cysteine-rich domains related to Frizzled receptors and Hedgehog-interacting proteins. Protein Sci *21*, 1172-1184.
Pilia, G., Hughes-Benzie, R.M., MacKenzie, A., Baybayan, P., Chen, E.Y., Huber, R., Neri, G., Cao, A., Forabosco, A., and Schlessinger, D. (1996). Mutations in GPC3, a glypican gene, cause the Simpson-Golabi-Behmel overgrowth syndrome. Nat Genet *12*, 241-247.
Roelink, H., Augsburger, A., Heemskerk, J., Korzh, V., Norlin, S., Ruiz i Altaba, A., Tanabe, Y., Placzek, M., Edlund, T., Jessell, T.M*., et al.* (1994). Floor plate and motor neuron induction by vhh-1, a vertebrate homolog of hedgehog expressed by the notochord. Cell *76*, 761-775.
Schmidt, C., Stoeckelhuber, M., McKinnell, I., Putz, R., Christ, B., and Patel, K. (2004). Wnt 6 regulates the epithelialisation process of the segmental plate mesoderm leading to somite formation. Dev Biol *271*, 198-209.
Serralbo, O., and Marcelle, C. (2014). Migrating cells mediate long-range WNT signaling. Development *141*, 2057-2063.
Shamim, H., and Mason, I. (1999). Expression of Fgf4 during early development of the chick embryo. Mech Dev *85*, 189-192.

Song, H.H., and Filmus, J. (2002). The role of glypicans in mammalian development. Biochim Biophys Acta *1573*, 241-246.
Veugelers, M., De Cat, B., Ceulemans, H., Bruystens, A.M., Coomans, C., Durr, J., Vermeesch, J., Marynen, P., and David, G. (1999). Glypican-6, a new member of the glypican family of cell surface heparan sulfate proteoglycans. J Biol Chem *274*, 26968-26977.
Wagner, J., Schmidt, C., Nikowits, W., Jr., and Christ, B. (2000). Compartmentalization of the somite and myogenesis in chick embryos are influenced by wnt expression. Dev Biol *228*, 86-94.
Wilson, N.H., and Stoeckli, E.T. (2013). Sonic hedgehog regulates its own receptor on postcrossing commissural axons in a glypican1-dependent manner. Neuron *79*, 478-491.
Ybot-Gonzalez, P., Copp, A.J., and Greene, N.D. (2005). Expression pattern of glypican-4 suggests multiple roles during mouse development. Dev Dyn *233*, 1013-1017.

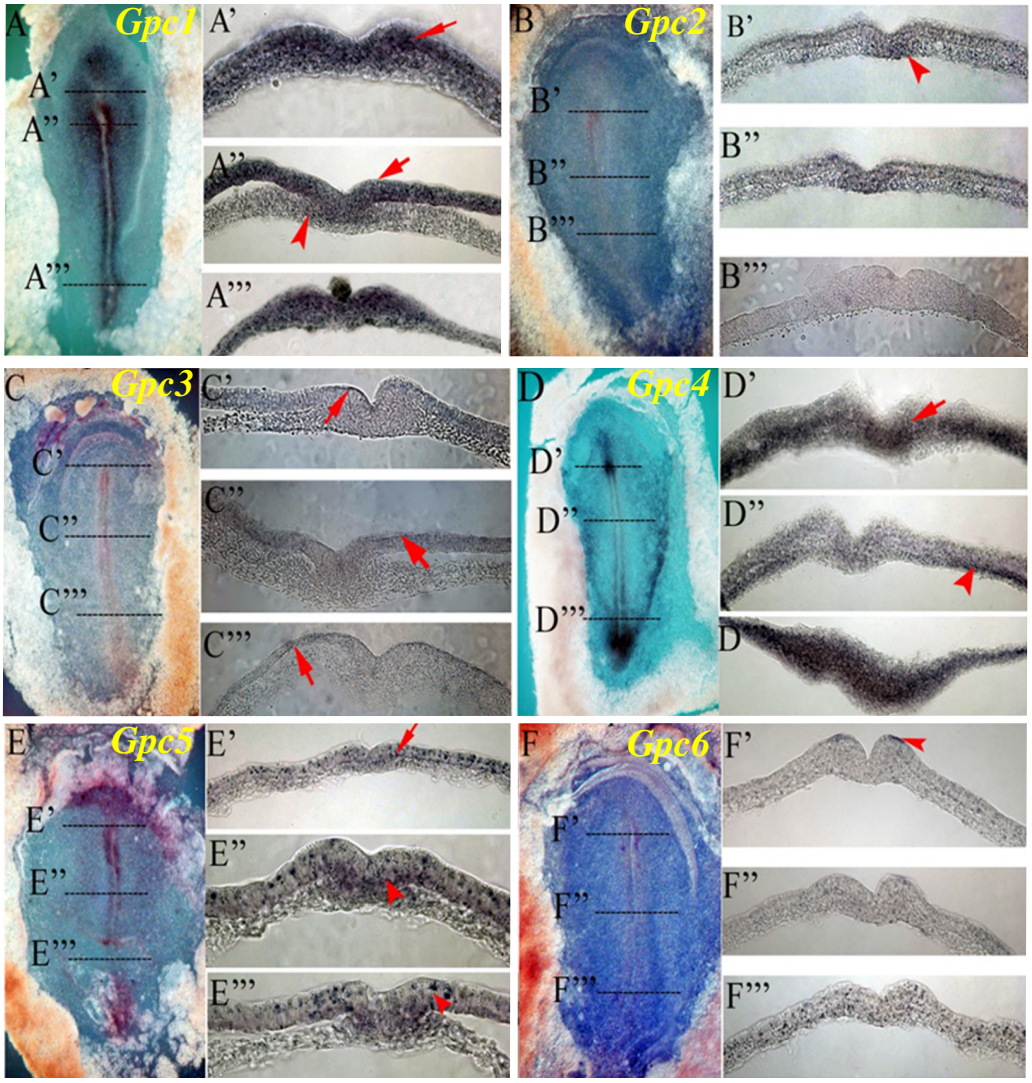
A
Gpc1
A'
A''
A'''
A'
A''
A'''
B
Gpc2
B'
B''
B'''
B'
B''
B'''
C
Gpc3
C'
C''
C'''
C'
C''
C'''
D
Gpc4
D'
D''
D'''
D'
D''
D
E
Gpc5
E'
E''
E'''
E'
E''
E'''
F
Gpc6
F'
F''
F'''
F'
F''
F'''

Fig 1

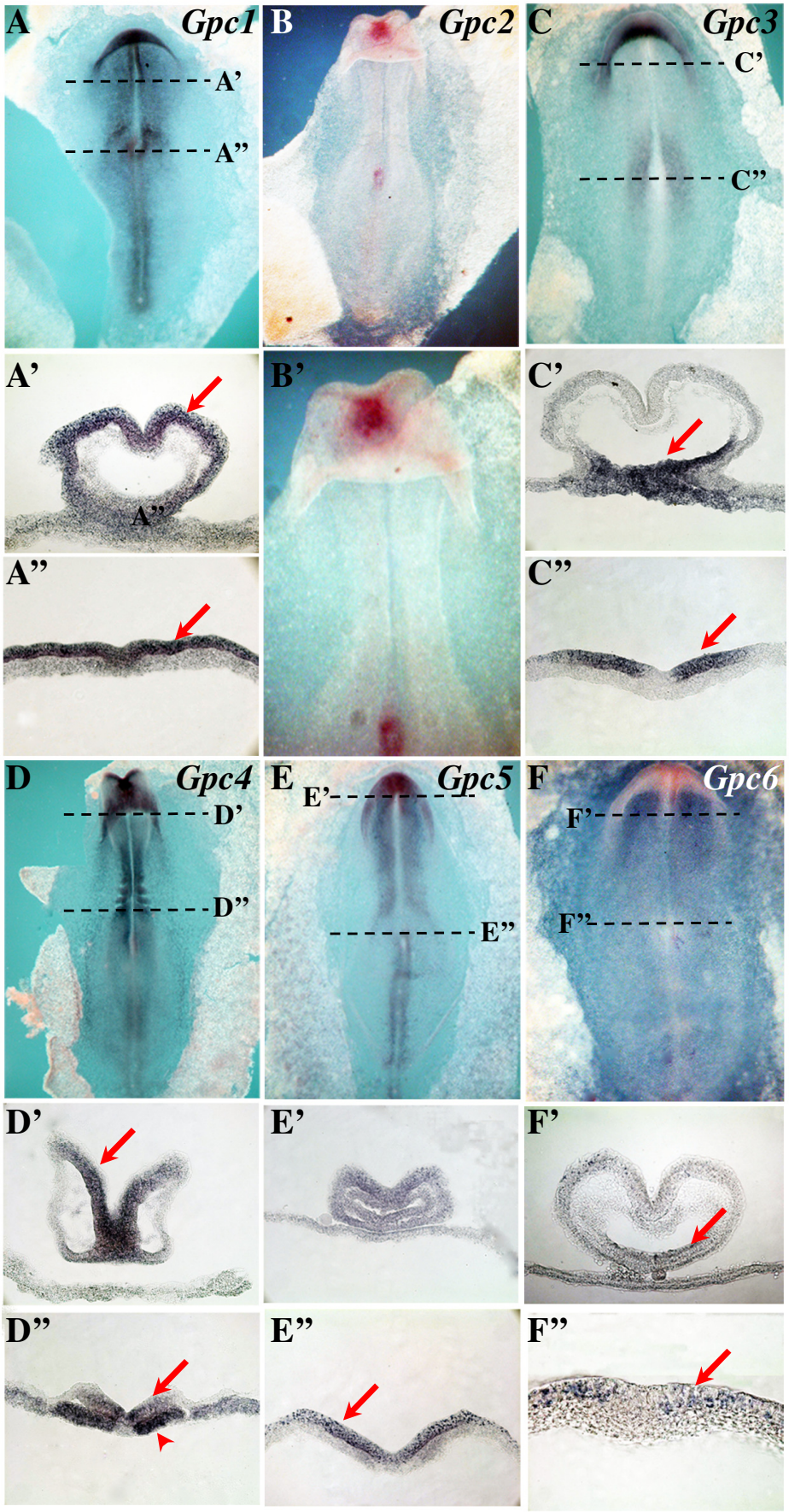
A
Gpc1
A'
A"
B
Gpc2
C
Gpc3
C'
C"
A'
A"
B'
C'
A"
C"
D
Gpc4
D'
D"
E
E'
Gpc5
E"
F
Gpc6
F'
F"
D'
E'
F'
D"
E"
F"

Fig 2

Fig 3

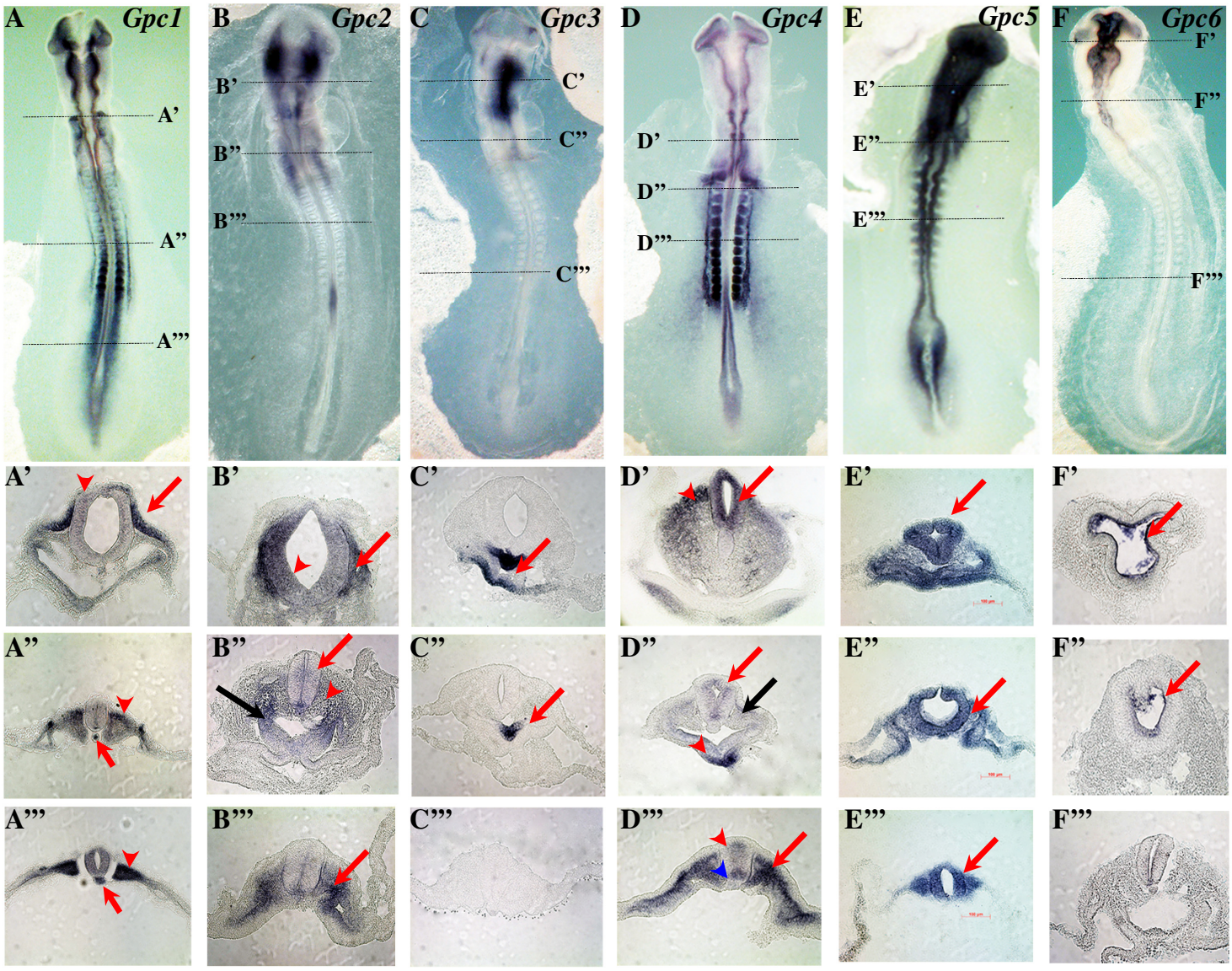
A
Gpc1
A'
A''
A'''
B
Gpc2
B'
B''
B'''
C
Gpc3
C'
C''
C'''
D
Gpc4
D'
D''
D'''
E
Gpc5
E'
E''
E'''
F
Gpc6
F'
F''
F'''
A'
B'
C'
D'
E'
F'
A''
B''
C''
D''
E''
F''
A'''
B'''
C'''
D'''
E'''
F'''

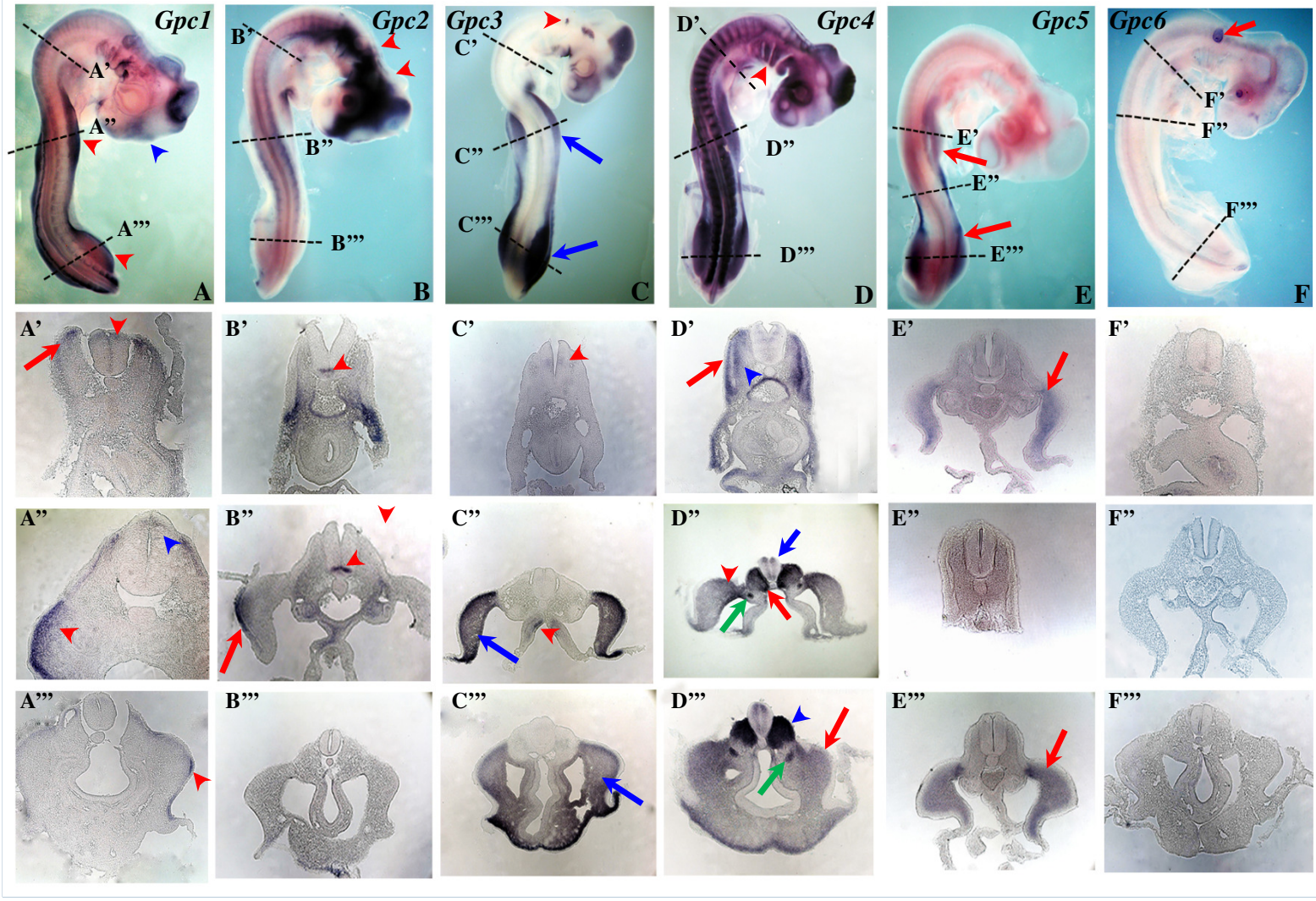

Fig 4

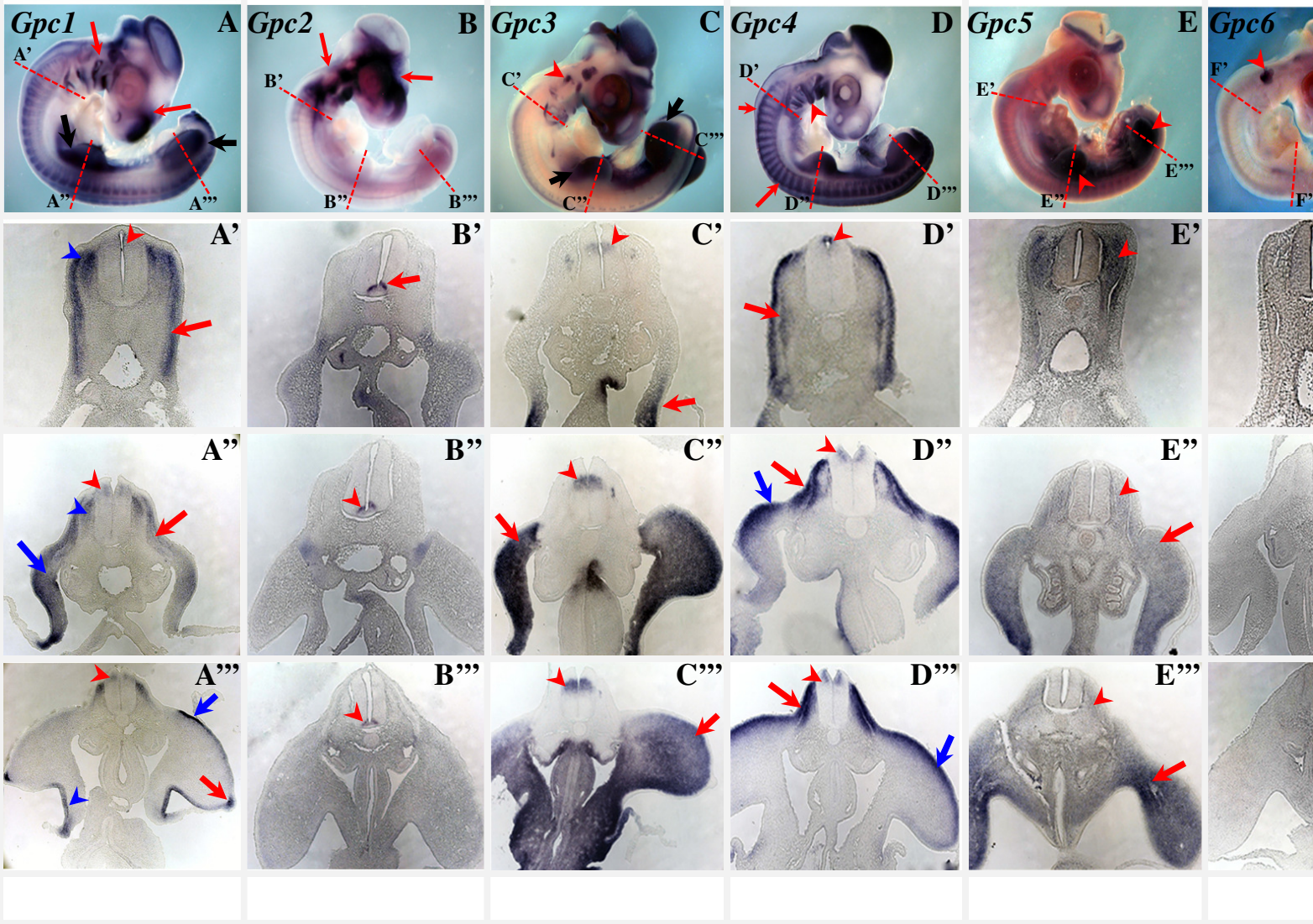
Gpc1
A
A'
A''
A'''
Gpc2
B
B'
B''
B'''
Gpc3
C
C'
C''
C'''
Gpc4
D
D'
D''
D'''
Gpc5
E
E'
E''
E'''
Gpc6
F'
F'
A'
B'
C'
D'
E'
A''
B''
C''
D''
E''
A'''
B'''
C'''
D'''
E'''

Fig 5

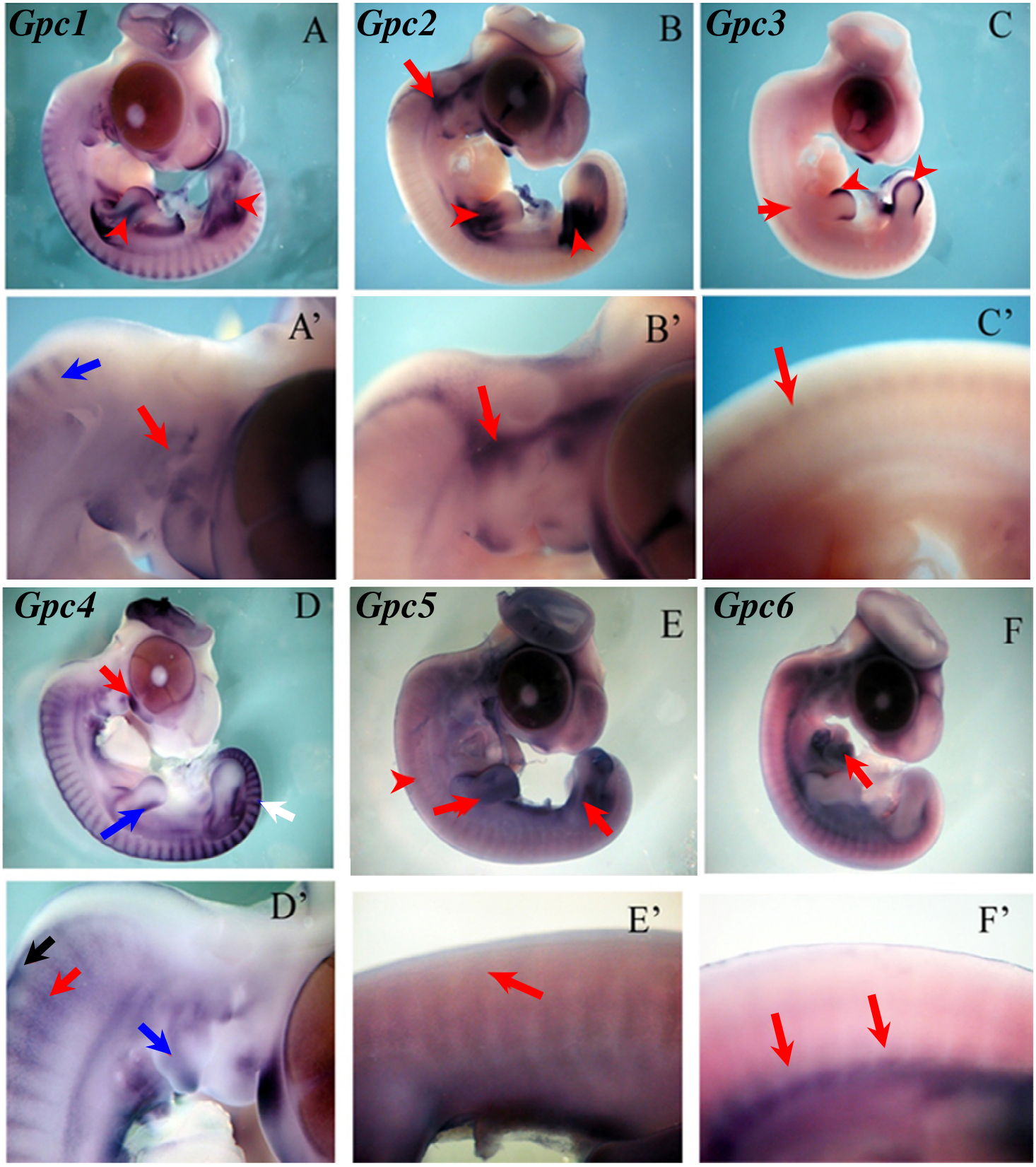

Fig 6

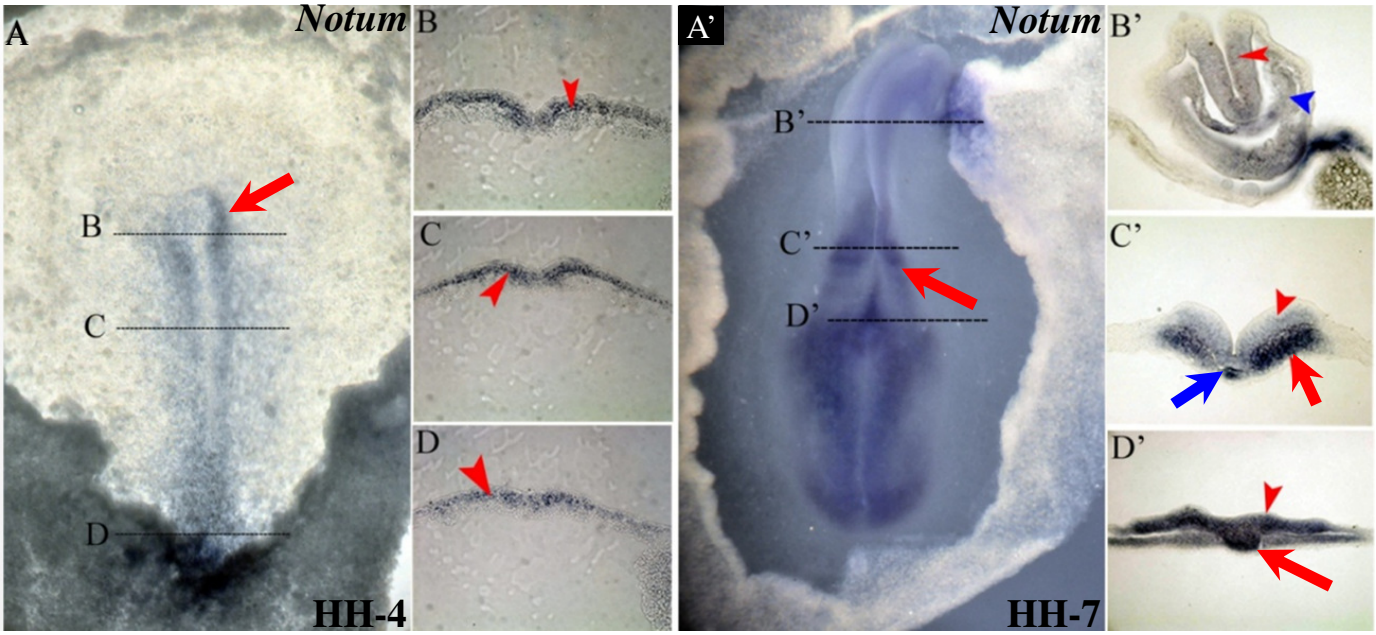

Fig 7

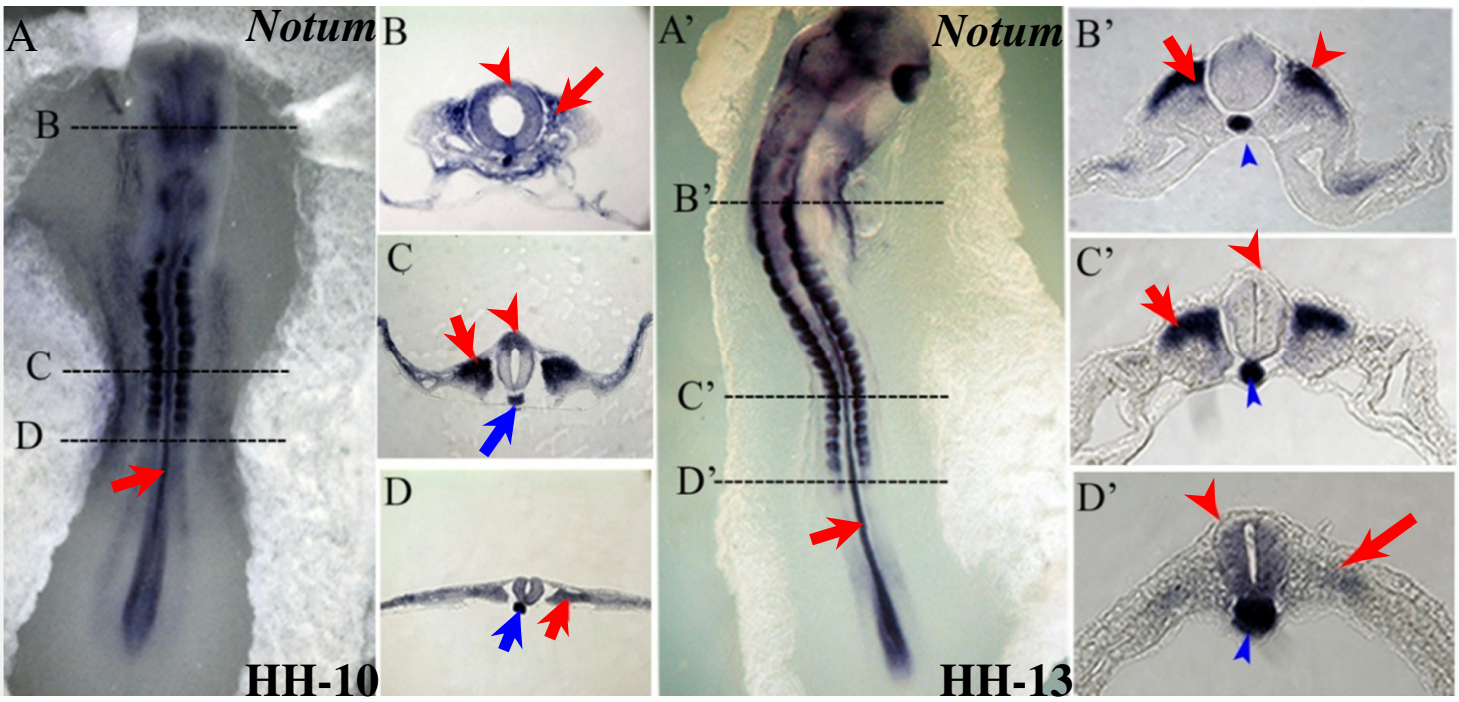

Fig 8

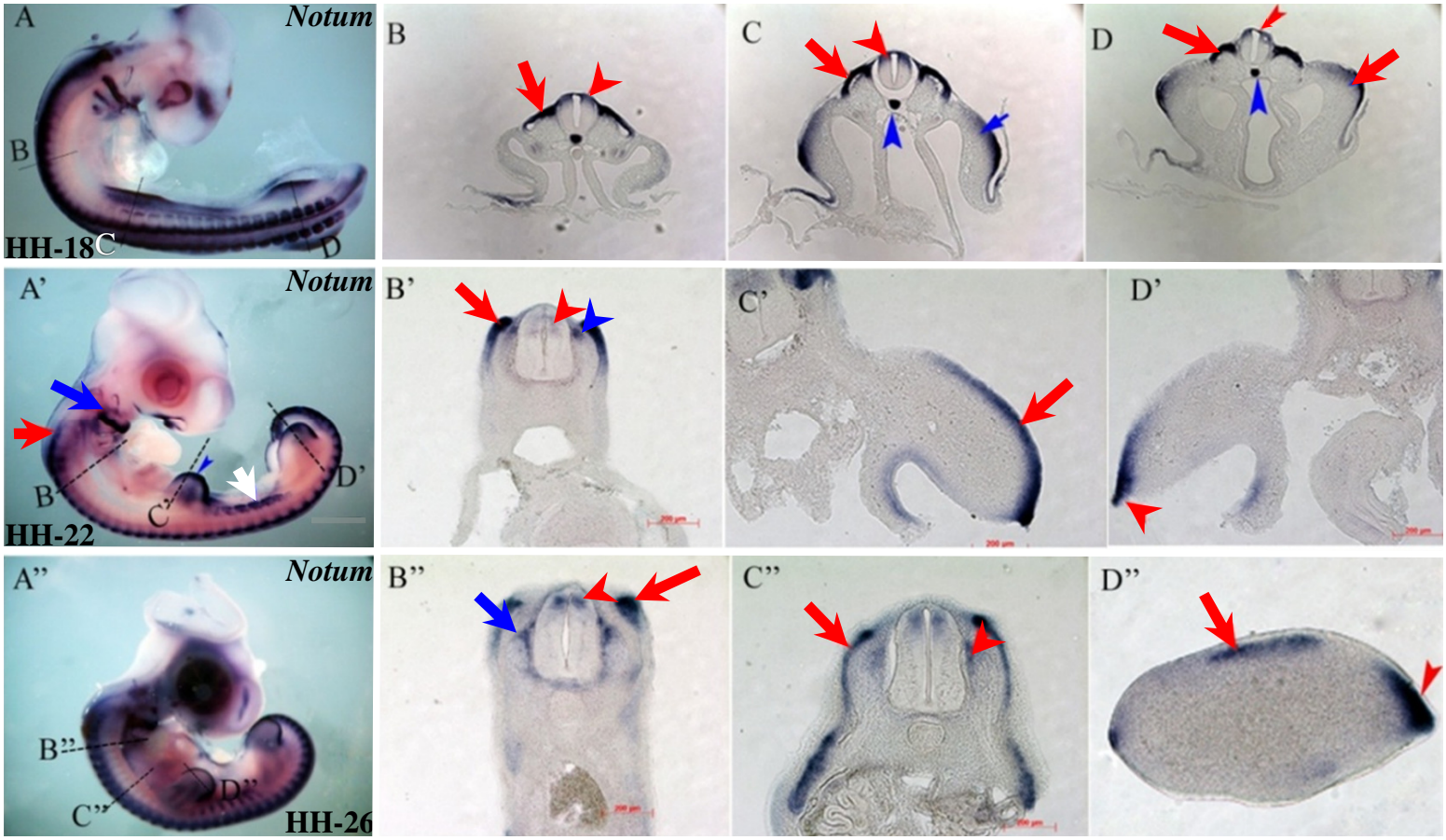

Fig 9

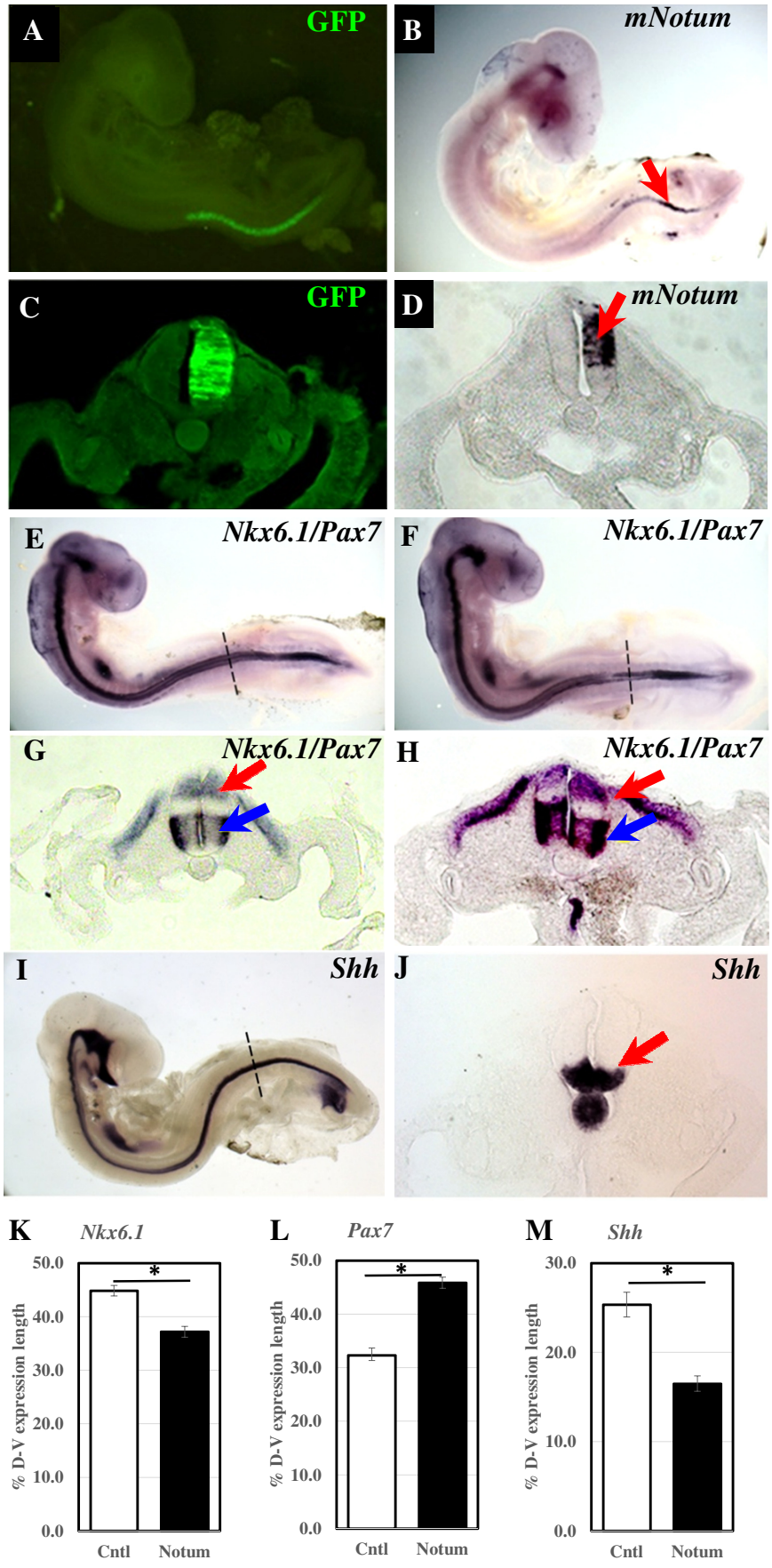
A
GFP
B
mNotum
C
GFP
D
mNotum
E
Nkx6.1/Pax7
F
Nkx6.1/Pax7
G
Nkx6.1/Pax7
H
Nkx6.1/Pax7
I
Shh
J
Shh
K
Nkx6.1
% D-V expression length
50.0
40.0
30.0
20.0
10.0
0.0
*
Cntl
Notum
L
Pax7
% D-V expression length
50.0
40.0
30.0
20.0
10.0
0.0
*
Cntl
Notum
M
Shh
% D-V expression length
30.0
20.0
10.0
0.0
*
Cntl
Notum

Fig 10